1-1-1988

# Molecular-Dynamics Simulation of the Structural Phase Transition in Rb$_2$CaCl$_4$

D. P. Billesbach
*University of Nebraska - Lincoln*

P. J. Edwardson
*University of Nebraska - Lincoln*

John R. Hardy
*University of Nebraska - Lincoln*

# Molecular-dynamics simulation of the structural phase transition in Rb₂CaCl₄

D. P. Billesbach, P. J. Edwardson, and J. R. Hardy

*Department of Physics and Astronomy, University of Nebraska–Lincoln, Lincoln, Nebraska 68588-0111*

We have simulated the structural phase transition of one member of $A_2BX_4$ layered perovskite-like compounds, $Rb_2CaCl_4$. This family of compounds may be thought of as being constructed from normal perovskite unit cells but with a different stacking arrangement. In recent months, this structural family has become extremely important since it is the parent structure from which the new class of high-temperature superconductors comes from. The simulation was done using *ab initio* potentials with no adjustable parameters. Our calculations show a specific-heat anomaly at 400 K which corresponds to an observed pseudorotation of the $CaCl_6$ octahedral group. This rotation is similar to the structural phase transitions observed in the perovskite-structure family. We also postulate a dynamically disordered high-temperature structure for this compound.

## I. INTRODUCTION

The class of compounds with formula $ABX_3$, known collectively as perovskites, are one of the most studied and well understood systems (in terms of their structural phase transitions) known.[1-4] There are families of compounds, very closely related to the perovskites, however, that have not been well studied. One of these is the layered compounds, prototypic of which is $K_2NiF_4$.[5-8] The importance of these compounds lies in the recent discovery of high-temperature superconductivity in doped forms of $La_2CuO_4$.[9,10] In this study, we have examined the structural phase transitions of one member of this structural class through computer simulation.

The perovskites in their high-temperature phase, consist of a cubic cage made of the $A$ cations which encloses an octahedrally coordinated $BX_6$ group as shown in Fig. 1. Many members of this structural group will undergo a structural phase transition which can be described as a pseudorotation of the $BX_6$ group about one or more of its axes.[4] The displacement is not a true rotation because the $B$—$X$ bond length perpendicular to the rotation axis changes to keep the $X$ ion in the cube face plane. It is obvious that in this structure there is a high degree of correlation between the $BX_6$ octahedra in all three crystal directions.

Examination of Fig. 2 shows that in the $A_2BX_4$ compounds the basic structural unit is still the perovskite cell. The difference between the two structural classes, then lies in the packing of the cells. In the perovskites, the cells are stacked one on top of another, with centers over centers. In the $A_2BX_4$ system, the cells are separated by a gap. Further, they are stacked with centers over corners. This produces, in contrast to the perovskites, a layered structure where the $BX_6$ units are strongly coupled to each other within the plane of the layer, but only weakly coupled to the units in neighboring layers.

In view of the preceding facts, we should expect similar types of structural phase transitions in the $A_2BX_4$ compounds to those seen in the perovskites. Because of the weak coupling in the $c$ direction, however, there should be some important differences as we have indeed seen to be the case.

## II. TECHNIQUE

In this study, we have used the method of constant-pressure molecular dynamics[11] to simulate the structural phase transitions in $Rb_2CaCl_4$. To do this, however, we must know the proper initial ionic configuration. This was arrived at through a static relaxation (minimization of the potential energy) of the lattice. When a local potential energy minimum was reached, the phonon frequencies and their corresponding eigenvectors were calculated at symmetry points in the Brillouin zone. In
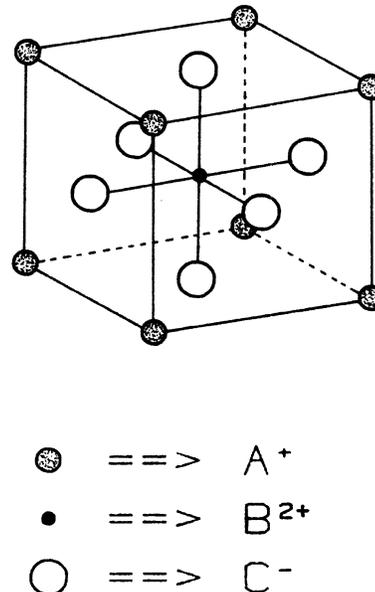


FIG. 1. $ABX_3$ perovskite structure.

most cases, there were some imaginary frequencies which corresponded to unstable displacement patterns. The most unstable of these displacement patterns was frozen in to the lattice and the potential-energy minimization was repeated. Through this iterative process, a completely stable lattice was obtained. This was our zero-temperature ground state and served as the starting structure for the molecular dynamics calculations.

The routine used to perform this simulation was essentially a standard molecular dynamics calculation. The major departure was in the inclusion of the lattice vectors as dynamic variables. This allowed the size and shape of the cell to change and gave a more realistic simulation of the structural phase transition.[11] The molecular dynamics calculation involved the solution of Lagrange's equations for the positions and velocities of all particles in the sample volume at discrete time intervals and for given amounts of total internal energy.

To solve Lagrange's equations, we must know all of the interionic potentials. In this study, we limited ourselves to completely ionic solids. That is to say, we assumed there was no electron sharing or covalent bonding in the system. We also 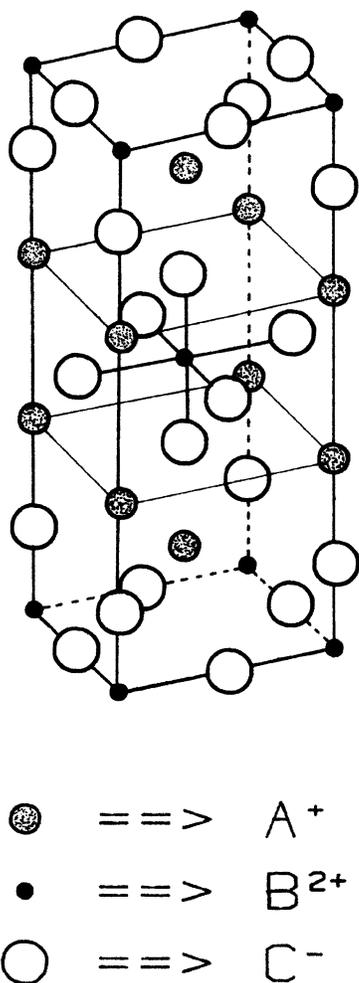restricted ourselves to ions with spherically symmetric charge densities. This required the solution of only a radial equation in the potential derivation and sped up the calculations considerably.

The long-range, Coulomb portion of the potential was calculated using the Ewald[12] summation technique and the short-range parts of the potentials were calculated using the technique of Gordon and Kim.[13] The initial charge densities were obtained from the tables of Clementi and Roetti.[14] After the potential was calculated at a suitable number of points, it was fitted to a function that could be analytically differentiated. The form of this function varied at different distances from the ion center. Innermost there was a hard, repulsive core potential given by

$$A + Br^{-6} .$$

In the intermediate region, the form was

$$r^k e^{-ar} \sum_n (c_n r^n), \quad n = 0-6 .$$

Finally, in the tail region, at large interionic separations:

$$Ce^{-Br^2}$$

These three forms and their first derivatives were matched where they joined to produce a smooth potential.

## III. MATERIALS

From the above discussion, there will obviously be some restrictions on which compounds can be studied by our methods. The most obvious of these is that the compound must be primarily ionically bonded. Furthermore, the constituent ions must remain spherically symmetric to a reasonable extent within the crystal field. It is also desirable to compare our results with any experimental data that may be available. These two conditions rule out compounds with transition metals in them such as $K_2NiF_4$ and the superconducting structures like $La_2CuO_4$. The $Ni^{2+}$ and the $Cu^{2+}$ would have an unfilled $d$ shell where the remaining electrons would most likely be somewhat loosely bound to the core and would tend to distort toward the cations. There is, however, a small amount of experimental data on the structure and phase transitions n $Rb_2CdCl_4$.[7,8] The presence of cadmium would be an obstacle in this compound for the same reasons, but if replaced by calcium, the simulation would be workable. In $Rb_2CdCl_4$, the cadmium is in a plus two charge state. If we compare the Pauling ionic radii of $Cd^{2+}$ with that of $Ca^{2+}$ we find that they are within two percent of each other. We thus can accept the substitution of $Rb_2CaCl_4$ for $Rb_2CdCl_4$. The phase transition temperatures obtained from the simulation will not be the same as those for the cadmium compound, but the general features of the transitions should match.

## IV. PROCEDURE

For our starting structure, we used the experimental lattice constants for the high-temperature phase of



$$\circledast \quad ==> \quad A^+$$

$$\bullet \quad ==> \quad B^{2+}$$

$$\bigcirc \quad ==> \quad C^-$$

FIG. 2.  $A_2BX_4$ layered perovskite structure. A perovskite cell has been outlined for clarity.

$Rb_2CdCl_4$.[7] The unit cell used was tetragonal with space group $I4/mmm$. This required two formula groups, or 14 ions per unit cell. This cell was relaxed with the constraint that the $I4/mmm$ symmetry be maintained. By doing this, we improved our initial guesses for the lattice vectors and relative ionic positions at little computational cost. Before starting the unconstrained relaxation, the cell was multiplied by two in all three crystal directions. This effectively mapped any cell doubling instabilities back to the zone center where the displacements were easy to freeze into the lattice. The new, larger cell now contained 112 ions and further static relaxations and lattice dynamical calculations required considerable central processing unit (CPU) time on a VAX 11/785 minicomputer. In our first attempts to relax this structure, we found instabilities at both the zone corner and on a zone edge. ($A$ and $M$, points respectively as seen Fig. 3.) These states represent points of unstable equilibrium on the potential energy surface. (Either maxima or saddle points.) To continue with the relaxation process, we had to induce the system to move to the next equilibrium point. The impetus was the addition of a small fraction of an unstable eigenvector displacement pattern to the ionic positions. When the $A$-point displacement was frozen in, the system relaxed immediately to a completely stable state with a potential energy of $-38.853$ eV per formula unit. It was found that if an $M$-point displacement was frozen in, the system first relaxed to an unstable state where the instability was found at the center of the top face of the zone. When this residual instability was frozen in, the lattice relaxed to an apparently stable state with a potential energy of $-38.826$ eV per formula unit. This apparently was not the ground state of the system since it lay at a higher energy than the $A$-point relaxed structure. We therefore chose the $A$-point relaxed cell as our ground-state structure. This structure was still tetragonal and had lattice vectors

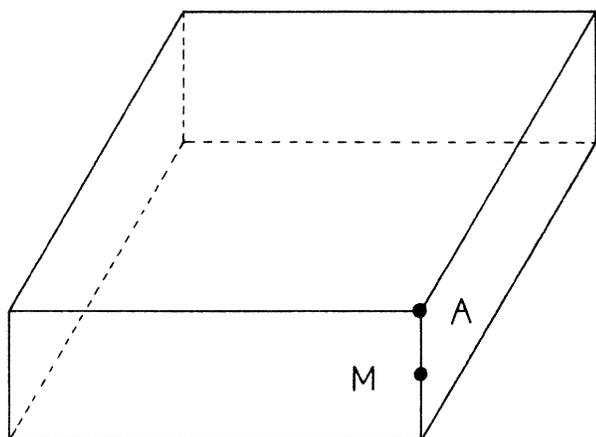$$a = b = 9.941 \text{ Å}$$

and

$$c = 33.041 \text{ Å} .$$



FIG. 3. Brillouin zone at the $A_2BX_4$ $I4/mmm$ phase showing the $M$ and $R$ symmetry points.

This structure was later thermodynamically verified by slowly cooling the system with the molecular dynamics program from a very high temperature.

Before the molecular dynamics routine was run on this structure, we desired to remove any residual kinetic energy from the lattice that may have been left over from the static relaxation and to assure ourselves that the system was truly in its ground state. To do this, a version of the molecular dynamics routine was used to quench the sample so that there was no kinetic energy left in the lattice. We note in passing that when the stable state reached from the $M$-point instability was quenched in this manner, its potential energy dropped to the same value as that of the true ground state, arrived at from the $A$-point instability. We then ran the molecular dynamics routine on this quenched ground state. In the first run, thermal energy equivalent to 50 K was added to the lattice between time intervals. The time intervals, during which the program collected data for the average velocities, positions, etc. were chosen to be 1.65 psec long. This was a long enough interval to include the effects of phonons with wave numbers 20 cm$^{-1}$ and greater. The program was allowed to step from 0 to 1000 K. To verify the results of this run, a second one was done with the same parameters, except that the temperature steps were cut in half to 25 K. At each temperature, the average ionic positions and their thermal ellipsoids were saved, as well as the cell side lengths, lattice vector angles, cell volume, and total kinetic and potential energies.

## V. RESULTS

Our molecular dynamics runs showed that there were no observable anomalies in the lattice vectors, their angles, or the cell volume. There was an anomaly in the specific heat however, along with a distinctive change in the ionic positions. Figures 4 and 5 show the specific heats calculated for the two runs. The anomalies are the bumps at 400 K. This bump appeared in both runs and had the same magnitude in both. In the first run, the anomaly is quite distinct. In the second run, it is somewhat hidden in noise, but is none the less present. These "noise" bumps were determined to be statistical fluctua-
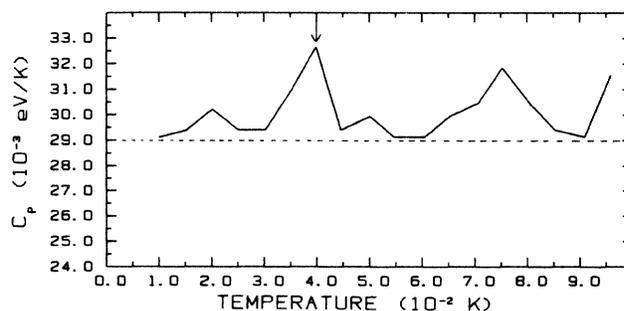


FIG. 4. Specific heat from the first run. The dotted line indicates the Dulong-Petit value for $C_P$ and the arrow indicates the anomaly.
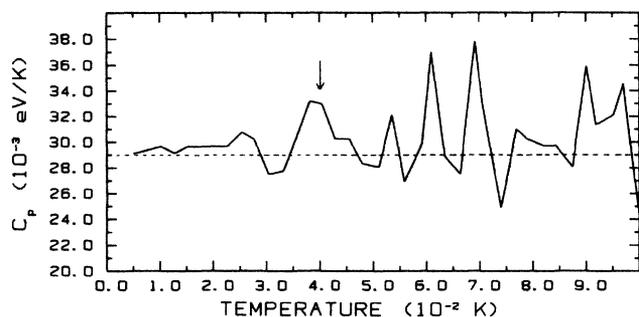
FIG. 5. Specific heat from the second run. The dotted line indicates the Dulong-Petit value for $C_p$ and the arrow indicates the anomaly.

tions which were the result of the small sample size. When the ionic positions were examined, it was found that parts of the sample were fluctuating between the two phases. We therefore believe that the first bump is an indicator of the transition onset. As a further test of the validity of the specific heat calculations, we compared the equilibrium values given in the graph with the harmonic value calculated from the Dulong-Petit relationship. This classical approximation to the specific heat for this sample is

$$C_p = 3nk_B = 0.028\,95 \text{ eV/K} ,$$

where $n$ is the number of particles in the sample and $k$ is Boltzmann's constant. The dotted lines in the figures indicate this value and it is plain that the simulation is in reasonable agreement with classical harmonic theory. This tends to support the reality of the specific heat anomalies, but to identify the phase transition unambiguously, we must examine the ionic displacements. Fig-
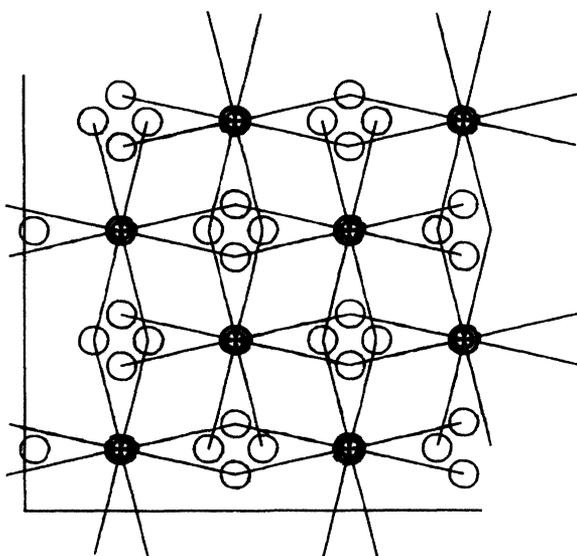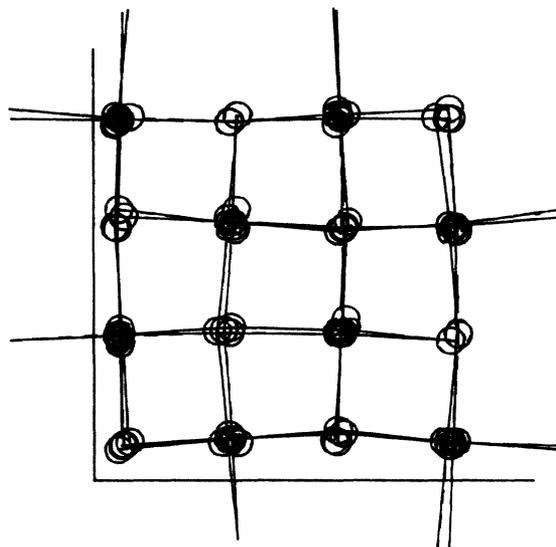


FIG. 7. View of the structure at 925 K, looking up the $c$ axis. The sizes of the circles are inversely proportional to the square root of the ionic mass.

ure 6 is a view from the first run of the structure at 51 K viewed up the $c$ axis. The pseudorotations of the $CaCl_6$ octahedra are quite apparent the $Cl^-$ ions have all shifted away from the high-temperature positions and now, instead of lining up on each other in this view, they form symmetric clusters. Figure 7 is another view from the first run, but at a temperature of 925 K. We see in this view, that the $Cl^-$ ions have apparently returned to the $I4/mmm$ symmetry or unrotated positions. To locate the phase transition, we must look at the patterns around 400 K. In Fig. 8 at 360 K, we still see the clus-
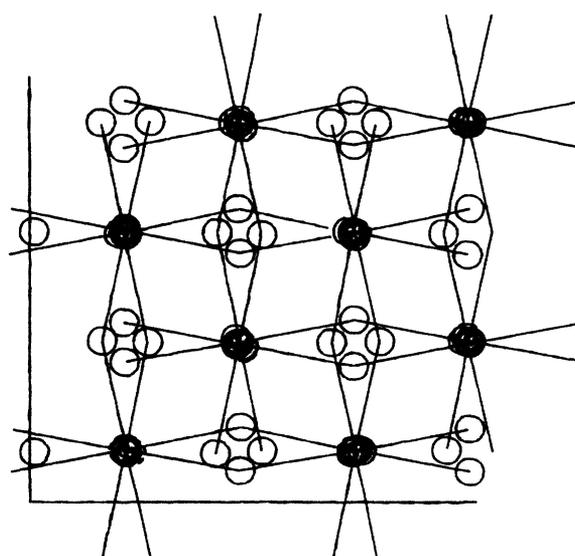


FIG. 6. View of the structure at 51 K, looking up the $c$ axis. The sizes of the circles are inversely proportional to the square root of the ionic mass.



FIG. 8. View of the structure at 360 K, looking up the $c$ axis. The sizes of the circles are inversely proportional to the square root of the ionic mass.

ters of $Cl^-$ ions indicating that the structure is in the low temperature or rotated phase. When we look at Fig. 9 at 405 K however, we see that the clusters have begun to "collapse" or rotate back to the high-temperature structure. We conclude both from this evidence and the specific-heat anomalies, that $Rb_2CaCl_4$ has undergone a structural phase transition at about 400 K. Furthermore, we see that the transition apparently involves only rotations of the $CaCl_6$ octahedra.

## VI. DISCUSSION

In discussing the results of this simulation, we want to compare and contrast them with the situation in perovskite structured crystals. In these, the main phase transitions also involve pseudorotations of the $BX_6$ octahedra.[4] These pseudorotations can be driven by lattice instabilities at either the $M$ point (middle of the zone edge) or the $R$ point (zone corner in the cubic structure). The $M$-point instability causes the cell to double in two directions and quadrupole its volume. By contrast, the $R$-point instability causes the cell to double in all three directions and octupole is volume. Because of the structural similarity between the perovskites and the $A_2BX_4$ compounds, we expected the $BX_6$ octahedra to behave similarly. The lattice dynamics has indeed verified this by simulating the same major instabilities as those found in the perovskites.

The lattice dynamical study also suggests that the phase transition is driven by an $A$-point instability (cell corner in the tetragonal structure). The difference between phase transitions driven by $A$-point and $M$-point instabilities will be in the sense of the octahedra rotations as viewed along the $c$ axis. The two types of transitions are shown schematically in Fig. 10. The $A$-point



FIG. 10. Schematic representation of $M$-point and A point driven transitions. The arrows indicate the directions of the pseudorotations of the $BX_6$ octahedra. Note that the A point structure has a doubled repeat length in the long direction when compared to the $M$-point structure.
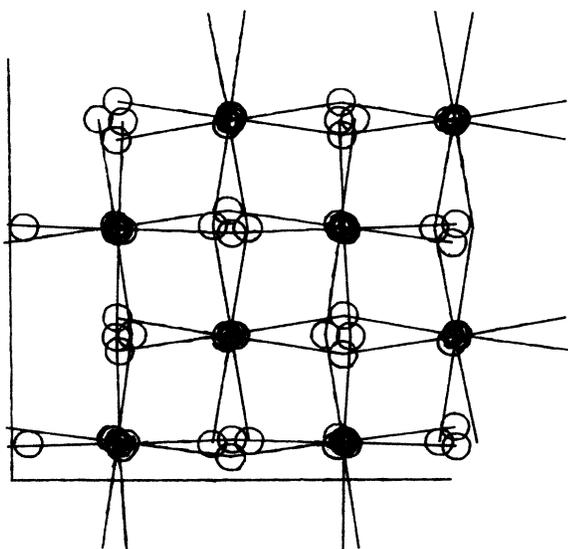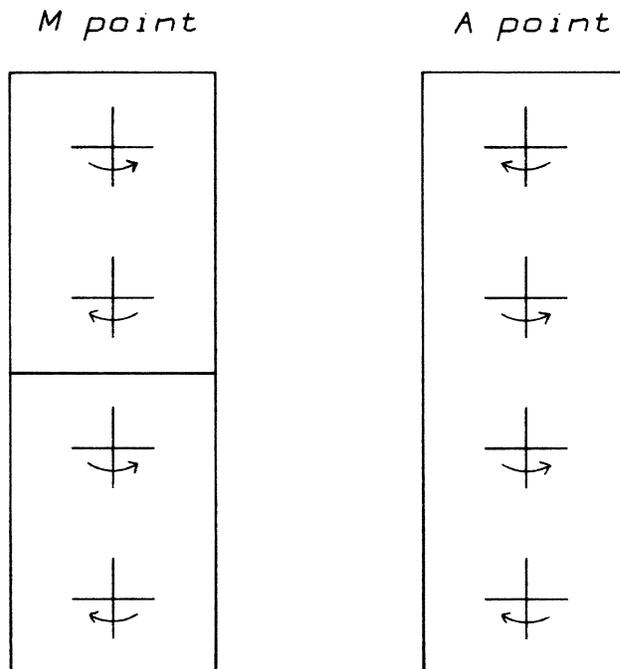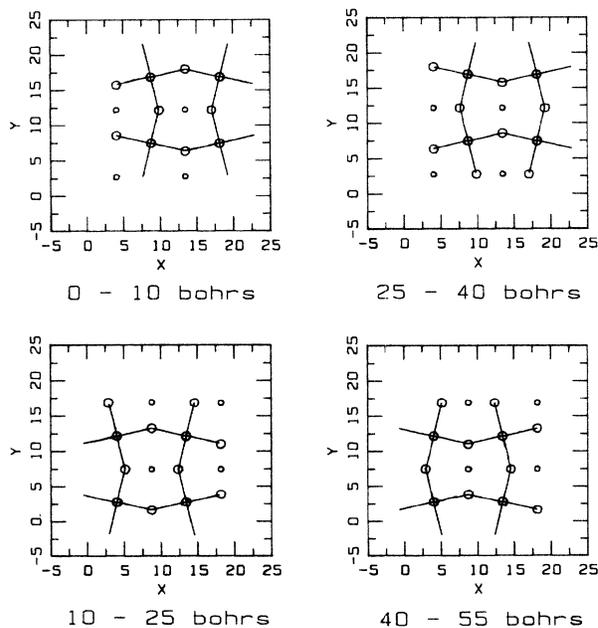




FIG. 9. View of the structure at 405 K, looking up the $c$ axis. Note the collapse of some of the $Cl^-$ clusters. The sizes of the circles are inversely proportional to the square root of the ionic mass.

FIG. 11. Individual sections in the $a$-$b$ plane at 51 K showing the $R$-point displacement pattern. Note, that this is the same data as in Fig. 6. The sizes of the circles are inversely proportional to the square root of the ionic mass.
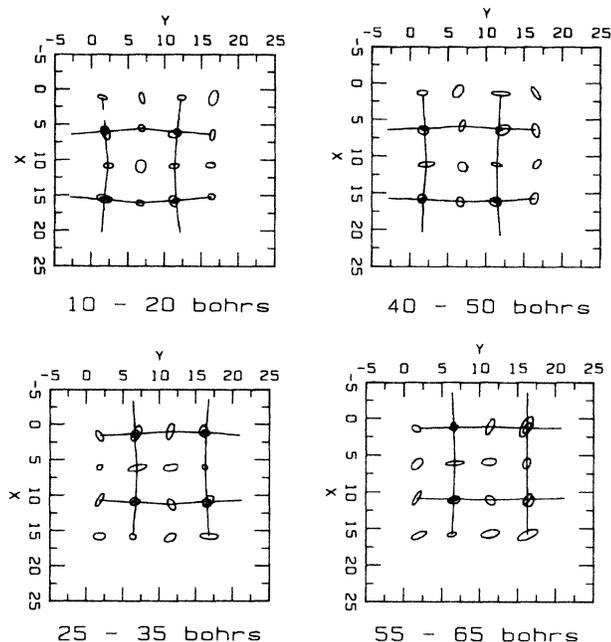
FIG. 12. Thermal ellipsoids for sections in the $a$-$b$ plane at 925 K.

instability plainly shows the cell doubling along the $c$ axis. The difference between the $A$-point and $M$-point instabilities can be described in terms of the stacking order of the pseudorotated octahedra along the $c$ axis. The $A$-point stacking order can be described as $AABB$ . . . packing while the $M$-point structure (which does not cause doubling along $c$) has a stacking order described as $ABAB$ . . . . If we look at sections perpendicular to the $c$ axis of the 51 K data, we see the patterns shown in Fig. 11. These clearly show the $AABB$ . . . stacking and confirm that this transition was driven by an $A$-point instability.

Another interesting feature of the simulation was the way in which the ions seem to move from the low-temperature to the high-temperature structures. The plots of the average ionic positions seem to show the $Cl^-$ ions not all moving to the high-temperature structure at the same time. In fact, there are some ions that appear to stay off of the high-temperature locations for several hundred degrees above the transition. We believe that there exist two almost identical occupation sites for the $Cl^-$ ions, one on either side of a line joining $Ca^{2+}$ ions. In the low temperature phase, the $Cl^-$ ions arrange themselves in these potential wells according to the $A$-point stacking order. In the high temperature phase, the $Cl^-$ ions will have enough thermal energy, to hop between the two sites. This hopping or dynamically disordered state would then show an average symmetry of $I4/mmm$, which is the high-temperature symmetry determined from x-ray studies.[8] In our simulation, the ionic displacement plots would not have good enough

statistics to show all $Cl^-$ ions at the high-temperature positions, especially near the transition temperature. Further evidence for this dynamically disordered model was seen in our plots of the thermal ellipsoids of the $Cl^-$ ions. As seen in Fig. 12, these plots show that the most probable locations of the $Cl^-$ ions in the high-temperature phase are in relatively large ellipsoids, elongated between the low-temperature positions.

Since $Rb_2CaCl_4$ has not, to the best of our knowledge, been studied experimentally, we have no real transition temperatures to compare with our simulation results. There is however, some work on $Rb_2CdCl_4$,[7,8] and since the $Ca^{2+}$ ion is almost the same size as the $Cd^{2+}$ ion, we may be able to extract some useful information from this work. We have already seen that the $BX_6$ octahedra may be expected to behave in a manner similar to that seen in the $ABX_3$ system. We therefore, will also look at the experimental work that has been done on $RbCaCl_3$ (Ref. 3) and on $RbCdCl_3$ (Ref. 15), i.e., the perovskite analogues of these two. Both of these compounds undergo similar phase transitions involving rotations to the $BX_6$ octahedra. The transition temperatures are

$$T_c = 573 \text{ K} \quad \text{for} \quad RbCaCl_3$$

and

$$T_c = 385 \text{ K} \quad \text{for} \quad RbCdCl_3 \ .$$

In the simplest approximation, we might expect the difference in transition temperatures between these compounds to be similar to the difference in transition temperatures between $Rb_2CaCl_4$ and $Rb_2CdCl_4$. If we subtract this difference from our simulation transition temperature of 400 K, we predict that $Rb_2CdCl_4$ should undergo a phase transition at about 212 K. In actual fact, the phase transition temperature in $Rb_2CdCl_4$ occurs at 142 K.[8] This is a discrepancy of 70 K which is probably in good agreement given the small statistical size of our simulation lattice and the fact that the $BX_6$ octahedra are different in the two systems: a difference that is only crudely approximated by the foregoing reduction of the transition temperature.

In summary, we believe that our *ab initio* calculations have realistically simulated one member of the $A_2BX_4$ layered perovskite family using purely ionic, parameter-free potentials. The simulation has yielded the expected structural phase transition and provided us with a reasonable result for the predicted phase transition temperature. Further, from the simulation results, we have been able to demonstrate the existence of dynamic disorder in the high-temperature phase.

[1]M. Hidaka, S. Maeda, and J. S. Storey, Phase Transitions 5, 219 (1985).

[2]A. Bulou, J. Nouel, A. W. Hewat, and F. J. Schafer, Ferroelectrics 25, 375 (1980).

[3]M. Midorikawa, A. Sawada, and Y. Ishibashi, J. Phys. Soc. Jpn. 48, 1202 (1980).

[4]J. W. Flocken, R. A. Guenther, J. R. Hardy, and L. L. Boyer, Phys. Rev. B 31, 7252 (1985).

[5]A. H. M. Schrama, Physica 68, 279 (1973).

[6]S. Ogawa, J. Phys. Soc. Jpn. 15, 1475 (1960).

[7]K. S. Aleksandrov, L. S. Emelyanova, S. V. Misjul, and I. T. Kokov, Solid State Commun. 53, 835 (1985).

[8]K. S. Aleksandrov, L. S. Emelyanova, S. V. Misjul, S. V. Melnikova, M. L. Gorev, I. T. Kokov, and A. D. Schafer, Jpn. J. Appl. Phys. Suppl. 24-2, 399 (1985).

[9]J. G. Bednorz and K. A. Muller, Z. Phys. B 64, 189 (1986).

[10]M. K. Wu, J. R. Ashburn, C. J. Torng, P. H. Hor, R. L. Meng, L. Gao, Z. J. Huang, Y. Q. Wang, and C. W. Chu, Phys. Rev. Lett. 58, 908 (1987).

[11]M. Parrinello and A. Rahman, Phys. Rev. Lett. 45, 1196 (1980).

[12]P. P. Ewald, Ann. Phys. 64, 253 (1921).

[13]R. G. Gordon and Y. S. Kim, J. Chem. Phys. 56, 3122 (1971).

[14]E. Clementi and C. Roetti, *Atomic Data and Nuclear Tables* (Academic, New York, 1974).

[15]S. V. Mel'nikova, A. T. Anistratov, and K. S. Aleksandrov, Fiz. Tverd. Tela (Leningrad) 23, 246 (1981) [Sov. Phys.—Solid State 23, 138 (1981)].